




Effect of marine heat waves on carbon metabolism, optical characterization, and bioavailability of dissolved organic carbon in coastal vegetated communities

Luis G. Egea ^{1*}, Rocío Jiménez-Ramos ^{1,2*}, Cristina Romera-Castillo,³ Isabel Casal-Porras,¹ Paula Bonet-Melià,⁴ Alba Yamuza-Magdaleno,¹ Lucía Cerezo-Sepúlveda,¹ José L. Pérez-Lloréns,¹ Fernando G. Brun ¹

¹Instituto Universitario de Investigación Marina (INMAR), Campus de Excelencia Internacional del Mar (CEI-MAR), Departamento de Biología, Facultad de Ciencias del Mar y Ambientales Universidad de Cádiz, Campus Universitario de Puerto Real, Puerto Real (Cádiz), Spain

²Institut Mediterrani d'Estudis Avançats, IMEDEA-CSIC, Mallorca, Spain

³Institut de Ciències del Mar, CSIC, Barcelona, Spain

⁴Instituto de Investigaciones Oceanológicas, Universidad Autónoma de Baja California, Mexico

Abstract

Dissolved organic carbon (DOC) plays an essential role in the global marine carbon cycle, with coastal vegetated communities as important DOC producers. However, the ultimate fate of this DOC remains still largely unknown due to the lack of knowledge about its chemical composition and lability. Furthermore, global change could alter both DOC fluxes and its bioavailability, affecting the carbon sequestration capacity of coastal vegetated communities. This study explores, in two contrasting seasons (winter and summer), the effects of an *in situ* simulated marine heatwave on carbon metabolism and DOC fluxes produced by seagrass (*Cymodocea nodosa*) and macroalgae (*Caulerpa prolifera*) communities. In addition, the fluorescent characteristics and biodegradability of the dissolved organic matter released directly by the communities under such conditions are evaluated. Under marine heatwave conditions, a significant increase in net community production (NCP) in *C. nodosa* and a shift to negative DOC fluxes in *C. prolifera* were observed. In control treatments, the seagrass-dominated community produced a substantial amount of labile (between 44% and 58%) and recalcitrant DOC (between 42% and 56%), while *C. prolifera* community produced mainly recalcitrant DOC (between 64% and 87%). Therefore, this research revealed that temperature is an important factor determining the NCP in benthic communities and the chemical structure and bioavailability of DOC produced by these communities, since both communities tended to produce more humic-like and less bioavailable DOC with increasing temperature.

*Correspondence: gonzalo.egea@uca.es, rocio.jimenez@uca.es

This is an open access article under the terms of the [Creative Commons Attribution-NonCommercial-NoDerivs](https://creativecommons.org/licenses/by-nc-nd/4.0/) License, which permits use and distribution in any medium, provided the original work is properly cited, the use is non-commercial and no modifications or adaptations are made.

Additional Supporting Information may be found in the online version of this article.

Author Contribution Statement: L.G.E. involved in conceptualization, investigation, methodology, data curation, formal analysis, funding acquisition, writing—original draft, writing—review and editing. R.J.-R. involved in conceptualization, methodology, data curation, formal analysis, funding acquisition, writing—original draft, writing—review and editing. C.R.-C. involved in conceptualization, formal analysis, data curation, writing—review and editing. I.C.-P., P.B.-M., A.Y.-M., and L.C.-S. involved in methodology, writing—review and editing. J.L.P.-L. and F.G.B. involved in conceptualization, funding acquisition, writing—review and editing.

The effect of warming on marine ecosystems has been studied for decades, but the effects of extreme climate events, such as marine heatwaves, are now highlighted as a major risk to marine ecosystems as a consequence of the reduced ability of species to withstand unexpected events rather than gradual temperature increases (Wernberg et al. 2013). Marine heatwaves are usually defined as a prolonged, discrete, anomalously warm water event that can be described by its duration (at least 3 d) and intensity (warmer than the 90th percentile of the local long-term climatological observations; typically at least 2°C) and that can occur throughout the year, even in winter (Hobday et al. 2016; Oliver et al. 2019). Seagrasses and benthic macroalgae are considered ecosystem engineers who provide a large number of ecological functions and services, including, for example, shoreline protection, suitable breeding habitats, biodiversity hotspots, and carbon sequestration

(Campagne et al. 2015; Jiménez-Ramos et al. 2021). In recent years, the effect of sudden and temporary temperature increases, such as marine heatwaves, on these communities has been assessed. However, most previous papers are either laboratory studies (Deguette et al. 2022) or studies that reported widespread mortality or reduced abundance of individuals following marine heatwaves (Wernberg et al. 2013; Arias-Ortiz et al. 2018). To date, little attention has been paid to the effects of *in situ* experimental marine heatwaves, where unexpected responses may be recorded as a consequence of integrating the entire community (i.e., sediment, fauna, macroalgae, epiphytes, plankton, etc.) into the experimental design (Macreadie and Hardy 2018; Egea et al. 2019a).

Seagrasses have been recognized for their carbon storage potential, leading us to consider these communities as a key element for carbon sequestration in marine areas (i.e., blue carbon) (Nellemann et al. 2009; Kennedy et al. 2010). Like seagrasses, benthic macroalgal communities have also been recently suggested as an important contributor to carbon sequestration in marine sediments (Krause-Jensen and Duarte 2016). The ability of natural ecosystems to act as carbon sinks has usually been related to the huge deposits of organic carbon buried in sediments, which are mainly formed by belowground refractory biomass (Kennedy et al. 2010). However, recent studies have highlighted the importance of the recalcitrant fraction of the dissolved organic carbon (DOC) as an important carbon sink with potential climate regulating capacity (Jiao et al. 2010). DOC is one of the largest exchangeable organic carbon pools in the marine environment, being a central factor in the global carbon cycle (Hansell 2013). Recently, the relevance of DOC generated by macrophyte communities has been highlighted, as it is a significant fraction of their net community production (NCP) (e.g., represents up to 46% of the global seagrass NCP; Barrón et al. 2014) and is a critical component of the carbon exchange between communities (Krause-Jensen and Duarte 2016; Egea et al. 2019b).

Changes in environmental conditions can alter DOC fluxes, but most of our knowledge is limited to studies in freshwater habitats (Larsen et al. 2011; Godin et al. 2017), although recently some studies have shown that DOC release in seagrass populations is highly dependent on environmental factors, such as hydrodynamics (Egea et al. 2018a), nutrient load (Egea et al. 2020; Liu et al. 2020), or increasing temperature (Egea et al. 2019a). However, the ultimate fate of DOC released from vegetated coastal communities (i.e., consumed or sequestered in the long term) may depend not only on the amount, but also on its turnover time (Jiao et al. 2010; Hansell 2013). That is, a significant fraction of DOC (i.e., the labile fraction), consisting of bioavailable material such as carbohydrates, amino acids, and proteins, is rapidly consumed by bacteria (average lifetime ~ 0.001 years; Hansell 2013) transferring carbon through the food web and fully involved in carbon exchange between communities

(Navarro et al. 2004; Egea et al. 2019b). However, another fraction of DOC (i.e., recalcitrant fraction such as humic-like substances) is resistant to rapid microbial degradation (average lifetime from ~ 1.5 years (semi-labile) to $\sim 40,000$ years (ultra-refractory); Hansell 2013). This fraction may be sequestered in continental shelf sediments or in the deep sea, and thus may contribute to long-term carbon sequestration (Krause-Jensen and Duarte 2016; Jiménez-Ramos et al. 2022). Therefore, changes driven by natural and anthropogenic factors in the labile/recalcitrant ratio of DOC produced by benthic communities may have a large and significant effect on its ultimate fate, but this is still a research gap that needs to be addressed.

The optical properties (i.e., absorbance and fluorescence) of dissolved organic matter (DOM) have been used extensively to assess both the sources and behavior of different fractions of DOM in marine systems (Coble 1996; Coble et al. 1998). The fraction of DOM that absorbs light in the ultraviolet (UV) and visible wavelengths is referred to as colored DOM (CDOM) (Coble et al. 1998). The subfraction of CDOM that emits induced fluorescent light is termed fluorescent DOM (FDOM). Two main groups of fluorophores have been differentiated (Coble et al. 1998): protein-like substances, which are considered bioavailable and can contribute substantially to bacterial demand for carbon and nitrogen in marine systems, and humic-like substances, which have traditionally been considered photodegradable but resistant to bacterial degradation. Thus, when humic-like FDOM is not exposed to natural UV radiation, it can accumulate in the ocean on centennial to millennial time scales within the global conveyor belt (Yamashita and Tanoue 2008). Therefore, the protein- and humic-like fluorescence could be used as a proxy to estimate the labile/recalcitrant ratio of the DOC pool produced in macrophyte benthic communities.

The optical characterization and bioavailability of DOC produced by vegetated coastal communities are not yet fully understood. Previous observations in some seagrass systems suggested that DOC released by seagrasses would contribute little to the refractory fraction of DOC (Ferguson et al. 2017; Akhand et al. 2021). In contrast, other studies observed how seagrass meadows directly produce recalcitrant DOM, which is retained in the water column (Watanabe and Kuwae 2015). Similarly, the fate of DOC exuded by macroalgae is still poorly studied. Opportunistic macroalgal species often release highly labile and biodegradable DOC (Zhang and Wang 2017; Chen et al. 2020), while other species such as the kelp *Ecklonia cava* appear to release more recalcitrant DOC (Wada et al. 2008; Zhang et al. 2017). The optical characterization and bioavailability of DOC released by *Caulerpa* sp. is still unknown.

In this study, an *in situ* manipulative experiment was conducted in which a sudden, short-duration temperature increase (as a proxy for a simulated marine heatwave) was designed and replicated in two contrasting seasons (winter and summer) to address the response of two vegetated coastal

communities (one dominated by the seagrass *Cymodocea nodosa* and the other dominated by the macroalga *Caulerpa prolifera*) to a simulated marine heatwave. In addition, the labile/recalcitrant ratio and chemical composition of DOC produced by both communities were also evaluated for the first time under all experimental conditions. Therefore, we have presented a pioneering study that aims to understand how vegetated coastal communities cope with the effects of marine heatwaves and the contributions of DOC released by these ecosystems as an overlooked tool in Blue Carbon strategies.

Materials and methods

Study area

The study was conducted in a shallow macrotidal and sheltered embayment (3545 ha) in the Santibáñez salt marsh, in the inner part of Cádiz Bay, southern Spain (36.47°N; 6.25°W). The benthic community consisted predominantly of dense, monospecific stands of the seagrass *Cymodocea nodosa* Ucria (Ascherson) and the green rhizophyte *Caulerpa prolifera* (Forsskål) J. V. Lamouroux. These populations inhabit shallow areas, at a depth of approximately 1 m below the lowest astronomical tide. Climatically, it fits into a semi-warm subtropical thermal regime whose normal seawater temperature range varies between 9°C and 28°C, with an average annual rainfall of 593 mm. The freshwater input into the system is negligible, so the average salinity ranges between 34.1 and 35.6 PSU. In the water column, nutrient peaks usually occur in winter, with values up to 1.4 $\mu\text{mol L}^{-1}$ NO_2^- , 12 $\mu\text{mol L}^{-1}$ NO_3^- , 25 $\mu\text{mol L}^{-1}$ NH_4^+ , and 1.5 $\mu\text{mol L}^{-1}$ PO_4^{3-} (Tovar et al. 2000). For detailed information of the study area, see previous descriptions in Jiménez-Ramos et al. (2021) and Peralta et al. (2021).

In situ experimental set-up of a simulated marine heatwave

To test the effects of a short-term (110 h) marine heatwave on carbon metabolism and DOC fluxes in two seasons (i.e., winter and summer) and in two different communities (i.e., *C. nodosa* and *C. prolifera*), an *in situ* temperature-rise experiment was set up. The experiments were conducted in February 2019 and September 2019, hereafter referred to as winter and summer trials, as they correspond to the period of maximum and minimum macrophyte growth and production in the area (Egea et al. 2019b; Peralta et al. 2021). To better compare the two study periods, sampling days were chosen at each season with a similar tidal range as well as weather forecast (e.g., presence of clouds, no rain, wind, etc.) to reduce environmental variability. Although each community was dominated by macrophytes, it is actually an assemblage of several biological components, such as plankton, epiphytes, other macroalgae, fauna, and sediment microbes. Therefore, the results integrate the entire community as a way to recreate a more realistic approach. In each season, for each community,

three replicated benthic chambers (hereafter called incubators) were randomly placed for each treatment (control and high temperature) by scuba diving. The minimum distance between replicates was 6 m and the locations of both treatments were mixed in each benthic communities, avoiding any bias due to the location of the treatments (distance to coast, meadow density, etc.) (Fig. 1).

Incubators were similar to those used in previous studies analyzing carbon metabolism and DOC fluxes *in situ* (Egea et al. 2019b) and manufactured by ©Aquatic-Biotechnology (Spain). Incubators consisted of two parts: a rigid polyvinyl chloride cylinder (diameter = 20 cm; height = 17 cm) and a transparent polyethylene plastic bag (height \approx 37 cm; width \approx 33 cm) attached to a polyvinyl chloride ring (width = 4 cm). Both parts were joined by a silicone gasket and tightly held by four rubber bands (Fig. 1). The cylinders were inserted into the sediment (15 cm) 2 h before fitting the plastic bags to reduce the effect of sediment disturbance. In addition, all six high-temperature incubators had underwater heaters (Easyheater 100 W; height \approx 15.5 cm and width \approx 4.5 cm) attached to the rigid polyvinyl chloride ring, separated from it by 2.5 cm and about 5 cm from the seafloor to heat the water to about 3°C (above water temperature) during the experimental period (110 h). HOBO data loggers (UA-002-64) were placed within each incubator and on the bare sediment ($n = 3$) near the experimental incubators to record temperature (°C) and light (lumens m^{-2}) every 10 min throughout the experimental period. To transform lumens m^{-2} into $\mu\text{mol photons m}^{-2} \text{ s}^{-1}$, the most common conversion factor given in the literature for sunlight was used (1 lumen $\text{m}^{-2} = 51.2 \mu\text{mol photons m}^{-2} \text{ s}^{-1}$; Carruthers et al. 2001). The daily light dose was calculated using the average daily hours of light (photoperiod) in each season (10.75 and 12.38 h in winter and summer trials, respectively).

During the simulated marine heatwave experiment, two types of polyethylene plastic bags were used alternatively: (i) a gas-permeable bag, and (ii) an air-tight bag. First, the gas-permeable bags were used for the first 90 h of the *in situ* experimental heating, which helped to minimize the risk of oxygen over-accumulation during the light hours and anoxic conditions during the night. After the first 90 h of the *in situ* experimental heating, the gas-permeable bags were replaced with air-tight bags to achieve a complete isolation of the community and thus allow the study of changes in dissolved oxygen and DOC fluxes under simulated marine heatwave conditions. To minimize heat loss from the water in the high-temperature treatments during bag replacement, we changed the bags rapidly (< 1 min) just before sunset, when the water temperature naturally decreased. Each air-tight bag was provided with a sampling port located in the upper half of the bag (≈ 20 cm) to draw water samples. The walls of both bags (wall thickness ≈ 0.07 mm) were flexible enough to allow movement with hydrodynamics, preventing water stagnation. Light penetration measured by the HOBOS inside the incubators was approximately $99.15\% \pm 0.01\%$ of incident light outside

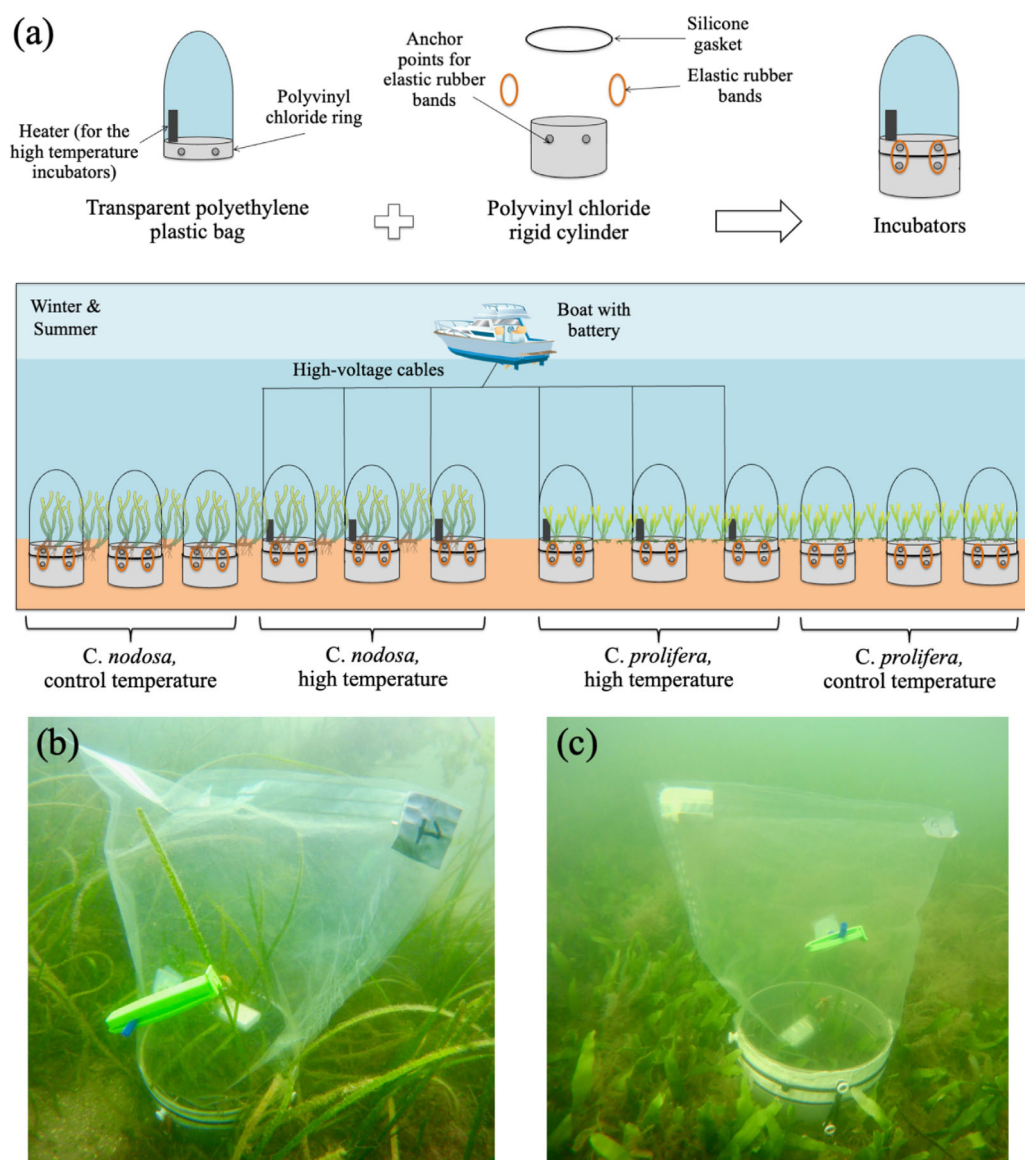


Fig. 1. (a) Simplified diagram of the incubators and experimental design. See detailed description in the text. The images show a representative in situ incubator in (b) *Cymodocea nodosa* and in (c) *Caulerpa prolifera* communities.

the bag. Oxygen diffusion controls were performed on the two types of plastic bags, showing oxygen permeability and oxygen nonpermeability of the plastic bags, respectively.

Simulated marine heatwave characteristics

Mean seawater temperature in control temperature treatments ranged from $15.6 \pm 0.07^\circ\text{C}$ in winter to $24.2 \pm 0.08^\circ\text{C}$ in summer. The heaters produced a steady temperature rise from ambient water temperature, and so the high-temperature treatments exhibited a temperature oscillation between day and night (Fig. 2). Seawater temperature in high-temperature treatments was statistically higher in both sampling events (about 3°C ; $p < 0.001$) compared to the control treatments, with a mean of $18.7 \pm 0.05^\circ\text{C}$ and $27.5 \pm 0.07^\circ\text{C}$ in winter

and summer, respectively. To assess the similarity of the temperature reached in the high-temperature treatments to the natural marine heatwaves in the area, the sea surface temperature (SST) and the occurrence of oceanic marine heatwaves close to Cádiz Bay were evaluated. The daily temperature dataset, displayed on the Marine Heatwaves Tracker app (Schlegel 2020), contains SST, climatology, threshold data, and the records of marine heatwave events from 1982 to present. A pixel near Cádiz Bay (Lon = 6.375°W , Lat = 36.375°N) was selected, and a time series of ocean SST was plotted from 08 June 2017 to 08 June 2022 (Supporting Information Fig. S1). The high-temperature treatments reached mean temperatures higher than the high SST threshold for the last 5 years in February ($16.3 \pm 0.03^\circ\text{C}$) and September ($24.4 \pm 0.03^\circ\text{C}$). In turn,

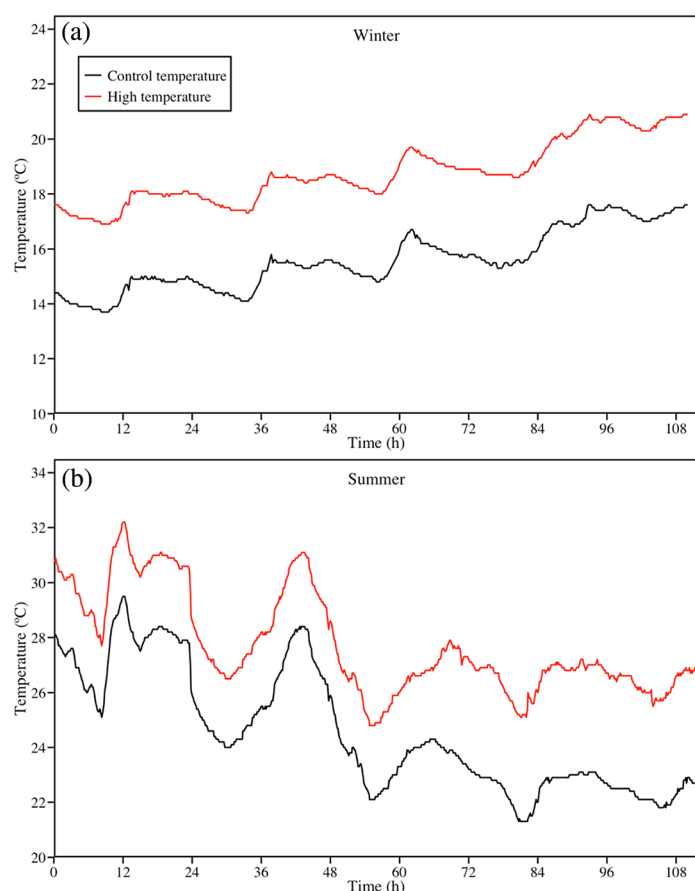


Fig. 2. Temperature–time series during the *in situ* experiment of the simulated marine heatwave. Lines are the mean of the control treatments ($n = 6$) (black) and high-temperature treatments ($n = 6$) (red), respectively.

17 marine heatwaves occurred in this period, lasting between 5 and 44 d and with an increase in SST between 1.21°C and 2.63°C. However, in shallow waters the temperature rise can be even higher than the average SST in marine areas (Deguette et al. 2022). Therefore, the increase of about 3°C reached in this experiment during 110 h was relevant to simulate a marine heatwave in the shallow water conditions of the Bay of Cádiz.

Sample procedure

Samples for community carbon metabolism (i.e., dissolved oxygen) and DOC fluxes were collected using acid-washed 50-mL syringes at three times during the last hours of the experimental period (on the 4th day): (i) just before sunset (S1), (ii) right after sunrise (S2), and (iii) 6 h after sunrise (S3). In this way, community carbon metabolism (through changes in dissolved oxygen concentration) and DOC fluxes in dark and light periods can be distinguished (Egea et al. 2019b). To calculate the exact water volume in each incubator, 20 mL of a 0.1 M uranine solution (sodium fluorescein, $C_{20}H_{10}Na_2O_5$) were injected into each incubator bag at the end of the simulated

marine heatwave experiment, allowing 15 min for mixing, and shaking the bag manually to facilitate rapid mixing of the uranine. The water samples were then collected and kept frozen until spectrophotometric determination according to Egea et al. (2019b). The mean volume of water enclosed in the incubator bags at the end of experimental period was 11.4 ± 0.2 L ($n = 24$).

Finally, upon disassembly of the experimental set-up, the macrophyte biomass within the incubators was harvested, rinsed and dried at 60°C to estimate the photosynthetic biomass (i.e., aboveground), subterranean biomass (i.e., belowground) and opportunistic macroalgal biomass (dry weight; $g\ DW\ m^{-2}$) of both communities. In this study, aboveground biomass of *C. prolifera* refers to fronds whereas belowground biomass refers to the subterranean network of cylindrical stolons with a series of rhizoid clusters, which is consistent with previous studies with this species (e.g., Vergara et al. 2012). For *C. nodosa*, aboveground biomass is shoots, while belowground biomass is rhizomes and roots (Brun et al. 2002). A fraction of the biomass was used to measure nonstructural carbohydrates (NSCs; i.e., sucrose and starch in aboveground and belowground tissues) following Brun et al. (2002).

Bioavailability assay of DOC produced by vegetated communities

At the end of the *in situ* simulated marine heatwave experiment and before removing the experimental set-up, 300 mL of seawater were taken from each incubator through the sampling port using acid-washed 50-mL syringes. The seawater collected was filtered and added to hermetic closure glass bottles at a ratio of 9 : 1 according to Jiménez-Ramos et al. (2022). For this purpose, 270 mL of water from the *in situ* incubators was filtered through a 0.2- μm polycarbonate filter into glass bottles. Bacterial cultures were then inoculated with the natural bacteria community collected in 30 mL of water from each *in situ* incubator and were filtered through a 0.8- μm polycarbonate filter to remove bacterial predators such as small flagellates. Incubation bottles ($n = 12$) were stored in darkness at 4°C until transported to the laboratory. Once in the laboratory, the DOC bioavailability assay was carried out for 7 d in a temperature-controlled room set at 18°C and under dark conditions, in accordance with previous works (Jiménez-Ramos et al. 2022). In this study, the term bioavailable/labile fraction of DOC refers to the fraction of DOC that is utilized by heterotrophic bacteria during the incubation time (i.e., 7 d). Likewise, we use the term recalcitrant fraction of DOC to refer to the remaining fraction of DOC. Ammonium (NH_4Cl) and phosphate (NaH_2PO_4) were supplied at the beginning to a final concentration of 10 and 2 μM , respectively, to avoid growth limitation by nitrogen or phosphorus availability. At time zero and every other days, samples were collected from each incubation bottle to measure DOC.

Carbon community metabolism analysis

Water samples for dissolved oxygen concentration from the simulated marine heatwave *in situ* experiment were fixed immediately after collection in the supporting vessel, kept in darkness and refrigerated, and determined using a spectrophotometric modification of the Winkler titration method (Pai et al. 1993; Roland et al. 1999). Hourly rates of community respiration (CR^h) and NCP (NCP^h) were calculated using the following formulas:

$$\text{CR}^h \left(\text{mmol O}_2 \text{ m}^{-2} \text{ d}^{-1} \right) = \frac{\text{DO}_{\text{S2}} (\text{mg O}_2 \text{ L}^{-1}) - \text{DO}_{\text{S1}} (\text{mg O}_2 \text{ L}^{-1})}{\frac{\Delta T_{T_{\text{S1}}-T_{\text{S2}}} (\text{h})}{\text{Vol} (\text{L})} \times \frac{1 (\text{mmol O}_2)}{32 (\text{mg O}_2)}} \times \frac{\text{Vol} (\text{L})}{\text{Area} (\text{m}^2)} \quad (1)$$

$$\text{NCP}^h \left(\text{mmol O}_2 \text{ m}^{-2} \text{ d}^{-1} \right) = \frac{\text{DO}_{\text{S3}} (\text{mg O}_2 \text{ L}^{-1}) - \text{DO}_{\text{S2}} (\text{mg O}_2 \text{ L}^{-1})}{\frac{\Delta T_{\text{S2}-\text{S3}} (\text{h})}{\text{Vol} (\text{L})} \times \frac{1 (\text{mmol O}_2)}{32 (\text{mg O}_2)}} \times \frac{\text{Vol} (\text{L})}{\text{Area} (\text{m}^2)} \quad (2)$$

$$\text{GPP}^h \left(\text{mmol O}_2 \text{ m}^{-2} \text{ d}^{-1} \right) = \text{CR}^h \left(\text{mmol O}_2 \text{ m}^{-2} \text{ d}^{-1} \right) + \text{NCP}^h \left(\text{mmol O}_2 \text{ m}^{-2} \text{ d}^{-1} \right), \quad (3)$$

where DO_{S1-S3} are the dissolved oxygen concentrations at sampling times S1-S3, ΔT is the elapsed time between sampling events, and “Vol” and “Area” are the volume and area of the incubators, respectively.

Finally, daily rates of community gross primary production (GPP^d), community respiration (CR^d), and NCP (NCP^d) were estimated following the calculations:

$$\begin{aligned} \text{GPP}^d &= \text{GPP}^h \times \text{Photoperiod} (\text{h}); \text{CR}^d = \text{CR}^h \times 24 \text{h}; \\ \text{NCP}^d &= \text{GPP}^d - \text{CR}^d, \end{aligned} \quad (4)$$

where photoperiod corresponds to the number of hours of sunlight measured on each sampling day.

Metabolic rates in units of dissolved oxygen were converted to carbon units assuming photosynthetic (PQ = moles O₂: moles CO₂) and respiratory quotients (RQ) of 1, a widely used value for benthic macrophyte communities (Tuya et al. 2014; Egea et al. 2019b).

DOC analysis

DOC samples from the *in situ* simulated marine heatwave experiment and the the produced DOC bioavailability assay were filtered through pre-combusted (450°C for 4 h) Whatman GF/F filters (0.7 μm) and kept with 0.08 mL of H₃PO₄ (diluted 30%) at 4°C in acid-washed material (encapsulated glass vials with silicone-PTFE caps) until analyzed. Concentrations of DOC were obtained by catalytic oxidation at high temperature (720°C) and chemiluminescence using a Shimadzu TOC-VCPH

analyzer. Certified reference material for DOC (low and deep), provided by D. A. Hansell and W. Chen (University of Miami), were used to assess the accuracy of the estimates.

Hourly rates of DOC production during the night and light periods in the *in situ* simulated marine heatwave experiment were calculated using the following formulas:

$$\begin{aligned} \text{DOC flux}_{\text{night}} \left(\text{mmol C m}^{-2} \text{ h}^{-1} \right) &= \frac{\text{DOC}_{\text{S2}} (\text{mg CL}^{-1}) - \text{DOC}_{\text{S1}} (\text{mg CL}^{-1})}{\Delta T_{T_{\text{S1}}-T_{\text{S2}}} (\text{h})} \times \frac{\text{Vol} (\text{L})}{\text{Area} (\text{m}^2)} \\ &\times \frac{1 (\text{mmol C})}{12 (\text{mg C})}, \end{aligned} \quad (5)$$

$$\begin{aligned} \text{DOC flux}_{\text{light}} \left(\text{mmol C m}^{-2} \text{ h}^{-1} \right) &= \frac{\text{DOC}_{\text{S3}} (\text{mg CL}^{-1}) - \text{DOC}_{\text{S2}} (\text{mg CL}^{-1})}{\Delta T_{T_{\text{S2}}-T_{\text{S3}}} (\text{h})} \times \frac{\text{Vol} (\text{L})}{\text{Area} (\text{m}^2)} \times \frac{1 (\text{mmol C})}{12 (\text{mg C})}, \end{aligned} \quad (6)$$

where DOC_{S1-S3}, are the DOC concentrations at sampling times S1-S3, ΔT is the elapsed time between sampling events, and “Vol” and “Area” are the volume and the area of the incubator, respectively.

Finally, daily rate of net DOC flux was estimated following the calculation:

$$\begin{aligned} \text{DOC} &= \text{DOC}_{\text{light}}^h \times \text{Photoperiod} (\text{h}) + \\ &\text{DOC}_{\text{night}}^h \times \text{Dark-period} (\text{h}), \end{aligned} \quad (7)$$

where photoperiod and dark-period correspond to the number of hours of sunlight and darkness measured on each sampling day.

Thus, when net DOC flux was positive, the community was considered to act as a net DOC producer (i.e., source). However, when net DOC flux was negative, the community was considered to act as a net DOC consumer (i.e., sink).

In the bioavailability assay of the DOC produced, the labile (DOC_L) and recalcitrant (DOC_R) fractions of the community DOC fluxes were calculated using the following formulas:

$$\begin{aligned} \text{DOC}_L &= \frac{\text{DOC}_{\text{initial}} (\text{mg L}^{-1}) - \text{DOC}_{\text{final}} (\text{mg L}^{-1})}{\text{DOC}_{\text{initial}} (\text{mg L}^{-1})}; \\ \text{DOC}_R &= \frac{\text{DOC}_{\text{final}} (\text{mg L}^{-1})}{\text{DOC}_{\text{initial}} (\text{mg L}^{-1})}, \end{aligned} \quad (8)$$

where DOC_{initial} and DOC_{final} are the DOC concentrations at the initial and final periods of the bacterial incubation assay.

Finally, the ratio between recalcitrant and labile DOC concentrations (DOC_R : DOC_L) at each sampling event was calculated as the recalcitrant DOC concentration (i.e., the DOC concentration at the end of the incubations with bacteria) divided by the labile DOC concentration (i.e., the difference between the initial and the final DOC concentrations during the incubations with bacteria) using the following formula:

$$\text{DOC}_R : \text{DOC}_L = \frac{\text{DOC}_{\text{final}} (\text{mgL}^{-1})}{\text{DOC}_{\text{initial}} (\text{mgL}^{-1}) - \text{DOC}_{\text{final}} (\text{mgL}^{-1})}. \quad (9)$$

FDOM analysis

FDOM samples from the *in situ* simulated marine heatwave experiments were filtered through pre-combusted (450°C for 4 h) Whatman GF/F filters (0.7 μm) and kept at 4°C in acid-washed material (glass vials encapsulated with silicone-PTFE caps) until analyzed. For FDOM analyses, excitation emission matrices (EEMs) were performed with a LS 55 PerkinElmer Luminescence spectrometer equipped with a xenon discharge lamp, equivalent to 20 kW for 8 ms duration. The detector was a red-sensitive R928 photomultiplier. Measurements were performed at a constant room temperature of 20°C in a 1-cm quartz fluorescence cell. The excitation wavelength ranged from 240 to 440 nm with 10 nm increments and the emissions wavelength from 300 to 560 nm at 0.5 nm increments, with excitation and emission bandwidths of 5 nm, and the integration time was 0.1 s (scan speed, 250 nm min⁻¹). The EEMs of the samples were corrected for Raman and Rayleigh scattering (Murphy et al. 2010) and normalized to the Raman area of the milli-Q water blanks. Raman area and its baseline correction were calculated from the emission scan of milli-Q water excited at 350 nm (Lawaetz and Stedmon 2009). Samples with an absorption coefficient at 254 nm greater than 10 m⁻¹ were diluted with MQ water to avoid inner-filter correction (Stedmon and Bro 2008). The drEEM 0.2.0 toolbox was used to standardize the EEMs (Murphy et al. 2013).

The changes in intensities of each peak were calculated during the dark period (i.e., the differences between S2 and S1) and during the light period (i.e., after extrapolating the differences between S3 and S2 for all daylight hours). Thus, the intensity changes at each peak during the whole day (24 h) were calculated by summing the hourly peak in daylight multiplied by the photoperiod and the hourly peak at night multiplied by the night hours using the following formula:

$$\text{Peak (RU)} = \frac{\text{Peak (RU)}_{S2} - \text{Peak (RU)}_{S1}}{\Delta T_{T_{S1}-T_{S2}} (\text{h})} \times \text{PP (h)} + \frac{\text{Peak (RU)}_{S3} - \text{Peak (RU)}_{S2}}{\Delta T_{T_{S2}-T_{S3}} (\text{h})} \times \text{NP (h)}, \quad (10)$$

where Peak_{S1}, Peak_{S2}, and Peak_{S3} are the intensity of peaks at different sampling times respectively, ΔT is the elapsed time between sampling events, PP (h) is the photoperiod and NP (h) is the night period.

Data and statistical analysis

The effects of treatment, community, and season on each response variable were tested using generalized linear models (GLMs). For each response variable, we selected a particular family error structure and link function to achieve the assumptions of linearity, homogeneity of variances and the

absence of overdispersion, which were checked by visual inspection of residuals and Q-Q plots (Harrison et al. 2018) after modeling. Aboveground biomass, belowground biomass, community biomass, opportunistic macroalgal biomass, GPP, CR, NSC content, and DOC bioavailability were modeled using Gamma distribution with inverse link, whereas NCP and DOC flux were modeled using Gaussian distribution with identity link. Pairwise comparisons were tested using estimated marginal means with a Bonferroni correction (“emmeans” R package; Lenth et al. 2019). A linear model was used to test the relationships between the main fluorescent peaks and temperature for each community and the relationships between humic-like peak-M and protein-like peak-T with GPP. Assumptions of normality and homoscedasticity were evaluated by examining the residuals of all linear models. Statistical analyses were computed with R statistical software 4.0.2 (R Development Core Team 2020).

Results

In situ marine heatwave simulated experiment

The simulated marine heatwave in *Cymodocea nodosa* produced a tendency to increase both CR and, especially, GPP (approximately 2.1 and 1.5 times higher in winter and summer, respectively), although differences were not statistically significant. As a result, the NCP increased significantly (i.e., approximately 1.9 and 1.7 times more than the control treatments in winter and summer, respectively) (Fig. 3). In contrast, the simulated marine heatwave in *Caulerpa prolifera* caused the opposite effect, showing a slight decrease in NCP as a consequence of a marked tendency to increase its CR (approximately 1.7 and 2.4 times higher in winter and summer, respectively), although differences were not statistically significant for this community (Fig. 3; Supporting Information Table S1).

DOC fluxes during daylight hours were higher than during night hours in *C. nodosa* ($p < 0.05$). Regarding *C. prolifera*, higher DOC release was found during night hours in the winter trial, whereas higher DOC release was recorded during daylight hours in the summer trial in the control treatments ($p < 0.05$). The simulated temperature increase shifted *C. prolifera* from DOC-consuming to DOC-producing during daylight hours in winter, whereas it shifted from DOC-producing to DOC-consuming during daylight hours in summer (Fig. 4a). In terms of daily DOC rates, both communities were DOC producers in the control treatments, especially *C. nodosa* in the winter trial. The simulated temperature increase raised the release of DOC in *C. nodosa* community (approximately 1.3 and 1.9 times more than the control treatments in the winter and summer trial, respectively) although no statistically significant differences were found. As for *C. prolifera*, the simulated temperature increase significantly reduced DOC fluxes in the summer trial to negative values, whereas a tendency to raise the daily DOC flux was found in winter (×2.7-fold), but without significant statistical difference (Fig. 4c; Supporting Information Table S2).

Aboveground biomass was significantly higher in summer than in winter in *C. nodosa* (average 111 ± 19 and 27 ± 5 g DW m⁻² respectively). In contrast, aboveground biomass was similar in *C. prolifera* in both seasons (average 32 ± 4 g DW m⁻²) (Supporting Information Fig. S2a). Aboveground biomass, belowground biomass, and community biomass (i.e., the sum of seagrasses, epiphytes and other opportunistic macroalgae) were similar between treatments in both communities and seasons (Supporting Information Fig. S2). A high proportion of opportunistic macroalgae (especially *Ulva* sp.) was found in *C. nodosa* in winter (average 71 ± 19 g DW m⁻², $\times 3.4$ higher than the average found in this community at summer and in the community dominated by *C. prolifera*) (Supporting Information Fig. S2d). As for NSCs content, they varied between macrophytes and seasons, but were not affected by increasing temperature in both communities (Supporting Information Fig. S3). Sucrose was the main NSC in *C. nodosa*, especially in belowground (rhizomes and roots) tissues, whereas starch was the main NSC in *C. prolifera*. *C. nodosa* increased its sucrose content in aboveground and belowground tissues in summer, while its belowground starch content decreased. No pattern was found between seasons in NSC content in *C. prolifera*.

Bioavailability assay of DOC produced by the vegetated communities

The DOC pool from the *C. nodosa* community experienced a sharp decline during the 1st 4–6 d after bacterial inoculation in the bioavailability assay (Supporting Information Fig. S4). The same was recorded for DOC from the *C. prolifera* community, but the decrease was milder. This initial phase of sharp decrease in the DOC concentration was followed by a final phase of stagnation in all the cultures. The lowest fraction of recalcitrant DOC flux (DOC_R) was found in *C. nodosa* in the winter control treatment (0.42), whereas the highest DOC_R was found in *C. prolifera* in the winter high-temperature treatment (0.92). All treatments showed DOC_R : DOC_L ratios higher than 1, except *C. nodosa* in the winter control treatment. The highest DOC_R : DOC_L ratios were found in the high-temperature treatments, especially for *C. prolifera* (Fig. 5; Supporting Information Table S3).

Optical characterization of the DOM produced

The main humic-like peaks observed in the EEMs of both communities were peak-A, peak-C, and peak-M (Fig. 6, Coble 1996). Peak-A was found at $< 240/400\text{--}450$ nm in all *in situ* incubators in summer, but shifted to Ex/Em $\sim 262/455$ nm in winter. Peak-C (usually categorized as terrestrial humic-like substances) and peak-M (usually described as marine humic-like substances) were found at Ex/Em $\sim 350/450$ nm and Ex/Em $\sim 320/420$ nm, respectively (Coble 1996). Since peak-A, peak-C, and peak-M presented a significant relationship between them (Pearson correlations $r \geq 0.6$; $p < 0.05$), only peak-C and peak-M data are shown in this study. As for the protein-

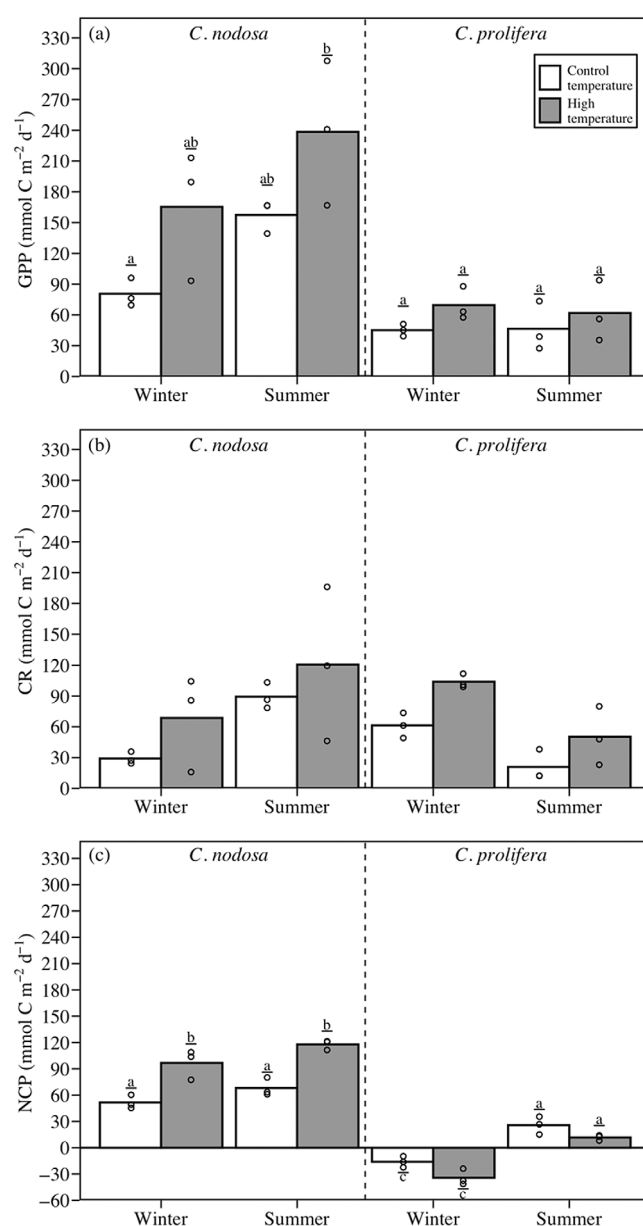


Fig. 3. Effect of an in situ simulated marine heatwave on (a) community GPP, (b) CR, and (c) NCP in communities dominated by *Cyrtocapsa nodosa* and *Caulerpa prolifera* in winter and summer. Different letters indicate significant differences among treatments, communities and seasons. Bars represent mean ($n = 3$) and dots represent the data.

like peaks, the peak-T maximum was observed at Ex/Em $\sim 280/375$ nm.

In winter, the control treatments of both communities showed a peak-C maximum around $\sim 360/450$ that shifted to shorter wavelengths (peak-M, $\sim 325/420$) with the simulated marine heatwave conditions. In summer, the main peak observed in the visible region was the peak-M for all treatments and communities. Also, a shift of the humic-like maxima in peak-C to peak-M was observed under higher

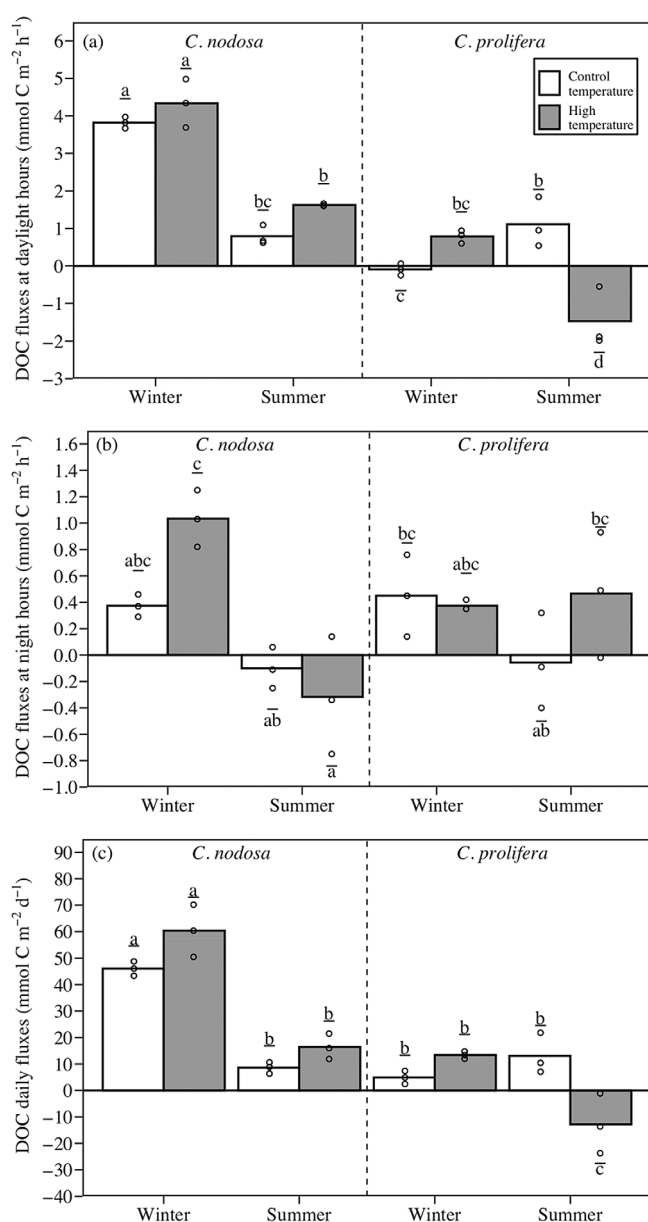


Fig. 4. Effect of an in situ simulated marine heatwave on (a) DOC fluxes in daylight hours, (b) DOC fluxes at night hours, and (c) daily DOC fluxes in communities dominated by *Cymodocea nodosa* and *Caulerpa prolifera* in winter and summer. Note the scale differences on the Y-axis. Different letters indicate significant differences among treatments, communities, and seasons. Bars represent mean ($n = 3$) and dots represent the data.

temperature conditions (i.e., high-temperature treatments in both seasons). Changes in the intensities of each fluorescent peak throughout the day (24 h) showed the pattern of FDOM consumption or production for each community and treatment (Supporting Information Table S4). Significantly higher FDOM intensity values were found in summer than in winter for both communities. The marine heatwave condition increased FDOM production in *C. nodosa* in summer. Meanwhile, increasing temperature appeared to elevate humic-like

peaks in the winter trial in *C. prolifera*, from being a consumer of humic-like peaks to a producer of humic-like peaks. The peak-T/peak-C ratio was less than 1 or negative in all treatments as a consequence of the peak-T consumption, except in *C. prolifera* in winter (Supporting Information Table S4).

A significant and positive linear regression ($p < 0.05$) was found between humic-like peaks with temperature (both natural, i.e., derived from seasonal temperature changes, and simulated, i.e., derived from the marine heatwave simulated in the experiment) for both communities (Fig. 7a,b). The linear regression between protein-like peak-T with temperature was significantly positive in the *C. nodosa*-dominated community but no significant regression was found in the *C. prolifera*-dominated community (Fig. 7c). A significant and positive linear regression ($p < 0.05$) was found between humic-like peak-M and protein-like peak-T with GPP in the *C. nodosa*-dominated community (Supporting Information Fig. S5). In contrast, no relationship has been found between FDOM and GPP in the *C. prolifera*-dominated community (Supporting Information Fig. S5).

Discussion

Effect of marine heat waves on vegetated community production

The simulated marine heatwave condition resulted in a significant increase in NCP in both seasons for the *Cymodocea nodosa*-dominated community, which is likely due to the enhanced photosynthetic rate. The optimum temperature for *C. nodosa* is higher than for other macrophyte species (up to 29.5°C; Savva et al. 2018) and temperature seems to favor enzymatic action in photosynthesis (Terrados and Ros 1995). In addition, the maximum quantum yield of photosystem II is also favored (Deguette et al. 2022) when the temperature increase is maintained within the thermal tolerance limits for this species (12.9–36.9°C; Savva et al. 2018; Egea et al. 2018b). This increase in photosynthetic rates and production with temperature has been demonstrated in other seagrass species such as *Halophila ovalis* (Collier et al. 2011) and *Zostera marina* (Marsh et al. 1986). High productivity in seagrasses may result in a high potential for substantial carbon burial rates (Duarte et al. 2013). Therefore, our results could suggest that a higher frequency of marine heatwaves in the coming decades could lead to an increase in net production of *C. nodosa*, which would add further arguments for the protection of this seagrass species, as they could sequester even more carbon under predicted conditions of climate change (i.e., higher temperatures and frequency of marine heatwaves). However, it should be noted that our results were obtained in a healthy community where *C. nodosa* reaches a high density and biomass, and inhabits sandy/muddy sediments with a medium organic matter content (2%) (Peralta et al. 2021). In other seagrass meadows where the canopy density was lower or the organic matter content in the sediment was higher, the effect

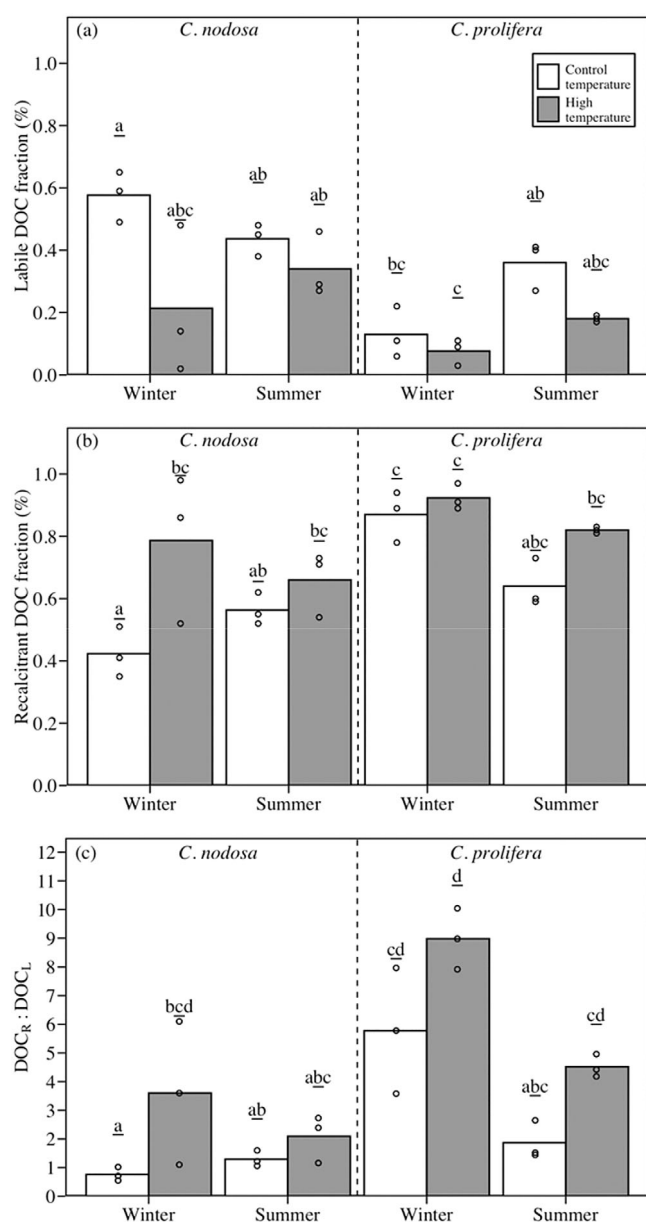


Fig. 5. (a) Labile DOC fraction, (b) recalcitrant DOC fraction, and (c) the recalcitrant DOC: labile DOC ratio in the different treatments, communities and seasons. Bars represent mean ($n = 3$) and dots represent the data.

of temperature on respiratory processes would probably gain more relevance (Malinverno and Martinez 2015), decreasing this potential carbon uptake. In addition, other seagrass communities growing near their thermal tolerance limit or under the effect of other limiting factors such as light or nutrients may show a different response than those recorded in this study (Arias-Ortiz et al. 2018). Therefore, the cumulative effects of several marine heatwaves on the growth and production of the seagrass community should be evaluated in future research. Unlike the *C. nodosa* community, the *Caulerpa prolifera* community did not show significant differences in both seasons,

although a trend of reduced NCP was observed, probably as a consequence of the higher rates of respiration than photosynthesis recorded in this species under higher temperatures (Terrados and Ros 1992). This trend is in line with previous studies that showed a decrease in the production of this macroalga in the summer period (Egea et al. 2019b) as a consequence of both high irradiance (Vergara et al. 2012) and elevated temperature (Vaquer-Sunyer et al. 2012).

Production values (i.e., GPP, CR, and NCP) in both communities in the control treatments were similar to those reported in the same area by Egea et al. (2019b), and similar to those reported by Duarte et al. (2010) for the seagrass and by Tuya et al. (2014) for the macroalga. The methodology used in this study has been widely utilized (Egea et al. 2019b) allowing for true independent replication and modification of a single factor (i.e., temperature), but it is not without methodological limitations. Because it is based on long-term incubations, pH and dissolved oxygen may differ from nearby natural meadows, where turbulent mixing prevents oversaturation during daylight hours and hypoxia during darkness (Champenois and Borges 2012). To address this, we used flexible gas-permeable bags for the 1st 90 h, which were replaced by air-tight bags on the last day to completely isolate the community. In our experimental set-up, the NCP was estimated for 6 h after sunrise, which may underestimate the NCP up to 25% (Olivé et al. 2016). As the DO concentrations measured in the S2 period were higher than the accepted threshold of 2 mg O₂ L⁻¹ for hypoxia (Vaquer-Sunyer and Duarte 2008), CR was probably not underestimated. Overall, it is possible that the NCP estimated in this study has some degree of underestimation as a result of the isolation of the community inside the incubator bag, indicating that these communities may be even more autotrophic than our results suggested.

Effect of marine heat waves on DOC fluxes

A substantial amount of autochthonous DOC was generated by both coastal vegetated communities derived from their high productivity, which is in agreement with previous studies (Watanabe and Kuwae 2015; Egea et al. 2019b). The values reported in the control treatments were within the range of values previously described for these species throughout the year in the area (Egea et al. 2019b) and similar to those reported by Barrón et al. (2014) (average of 12.4 ± 2.9 and 23.2 ± 12.6 mmol C m⁻² d⁻¹ for seagrass and macroalgae, respectively). The only exception were the slightly higher values found in winter in *C. nodosa*, which can be attributed to the high biomass values of opportunistic macroalgae present in the community, which probably elevated DOC production. Our results also showed that the *C. nodosa* meadow displayed higher net DOC release during sunlight hours than in darkness, when the community may even act as DOC consumer in the summer trial (Fig. 4). This is in agreement with previous studies in seagrasses (Barrón et al. 2014; Egea et al. 2019b), and suggests that a significant fraction of the

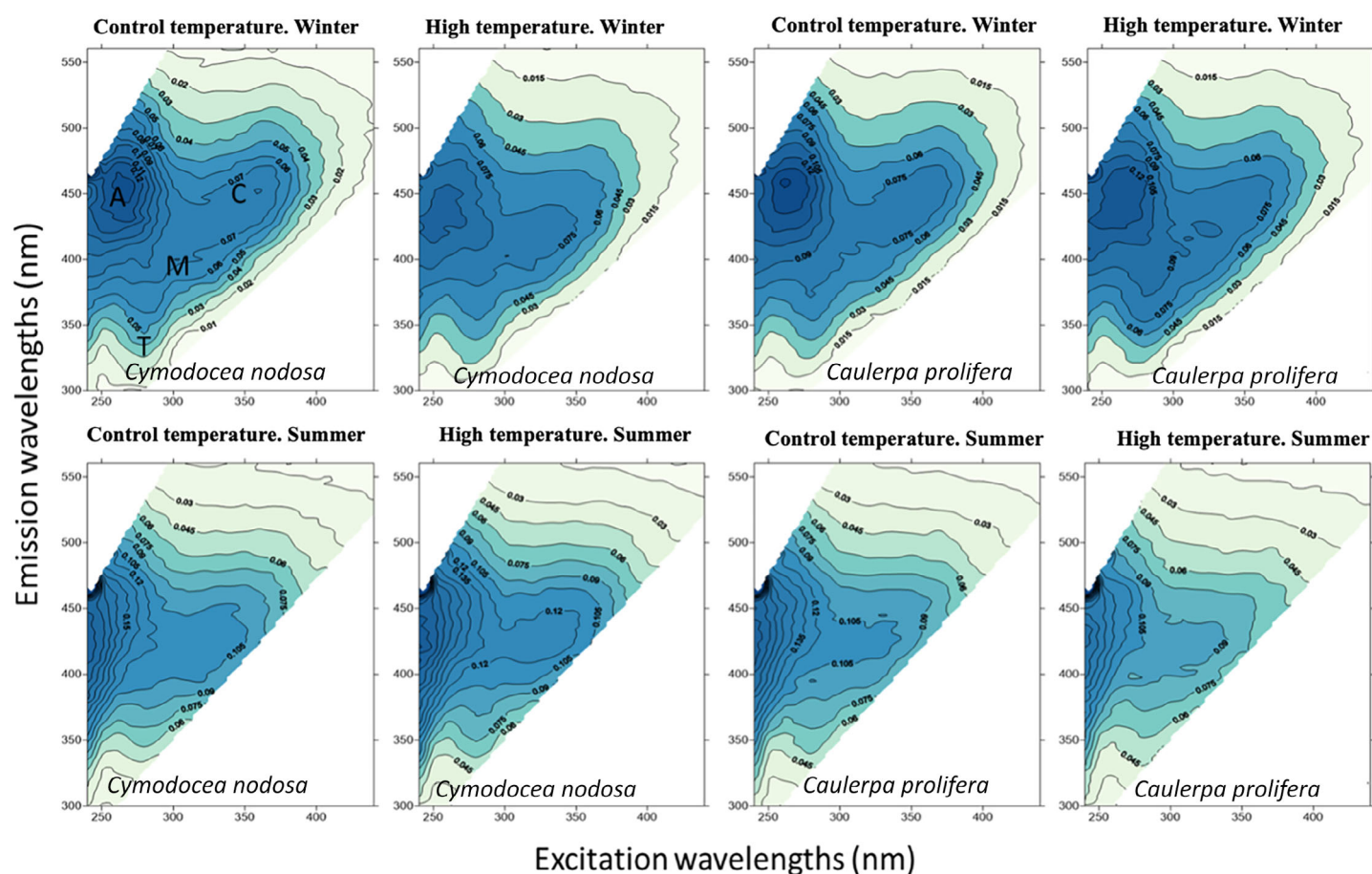


Fig. 6. FDOM EEMs of in situ incubators at the end of the marine heatwave experiment. Fluorescent intensity is reported in Raman units (R.U.). The main Coble's peaks are indicated in the 1st plot. Humic-like peaks are A, C, and M, while peak-T is classified as protein-like.

DOC released by this community is mostly done by photosynthesis activity. In contrast, *C. prolifera* acted as a DOC consumer during sunlight hours, which may suggest that the contribution of photosynthesis activity to DOC released by this community may not be as important. This is consistent with previous studies on other macroalgae such as kelps (Weigel and Pfister 2021) or rhodophytes like *Pyropia haitanensis* (Xu et al. 2022). Given that the higher organic matter content and smaller sediment grain size (i.e., muddy sediments) are typical in bottoms where this species thrives (Vergara et al. 2012), DOC release from POC remineralization in the sediment could also be more relevant in this community (Loginova et al. 2020).

Marine heatwave conditions significantly reduced the daily DOC flux in *C. prolifera* in summer, which became negative, whereas a tendency was found to increase the daily DOC flux in winter ($\times 2.7$ -fold but no significant statistical difference). These contradictory changes in DOC fluxes between the two trials could be explained by the role of other community components such as plankton, as the latter is an important DOC consumer from macroalgae, especially in summer (Egea

et al. 2019b). As for *C. nodosa*, marine heatwave conditions did not produce significant differences in both seasons, although there was a tendency to increase its daily DOC flux, especially in summer, when the DOC flux in high-temperature treatments doubled that of the control treatments, although differences were not statistically significant.

Bioavailability of DOC produced by vegetated communities

Overall, both communities showed a $DOC_R : DOC_L$ ratio > 1 in all seasons and treatments, indicating that both communities tend to release a higher proportion of recalcitrant DOC than labile fraction. The only exception was *C. nodosa* in the winter control treatment, which is likely related to the large biomass of opportunistic macroalgae (*Ulva* sp.) present in the community, which tend to release mainly labile and biodegradable DOC (Zhang and Wang 2017). The *C. nodosa*-dominated community released a similar proportion of recalcitrant (DOC_R ; 42% in winter and 56% in summer) and labile fraction (DOC_L) in control treatments. The high DOC_L fraction found here explains the close coupling between DOC

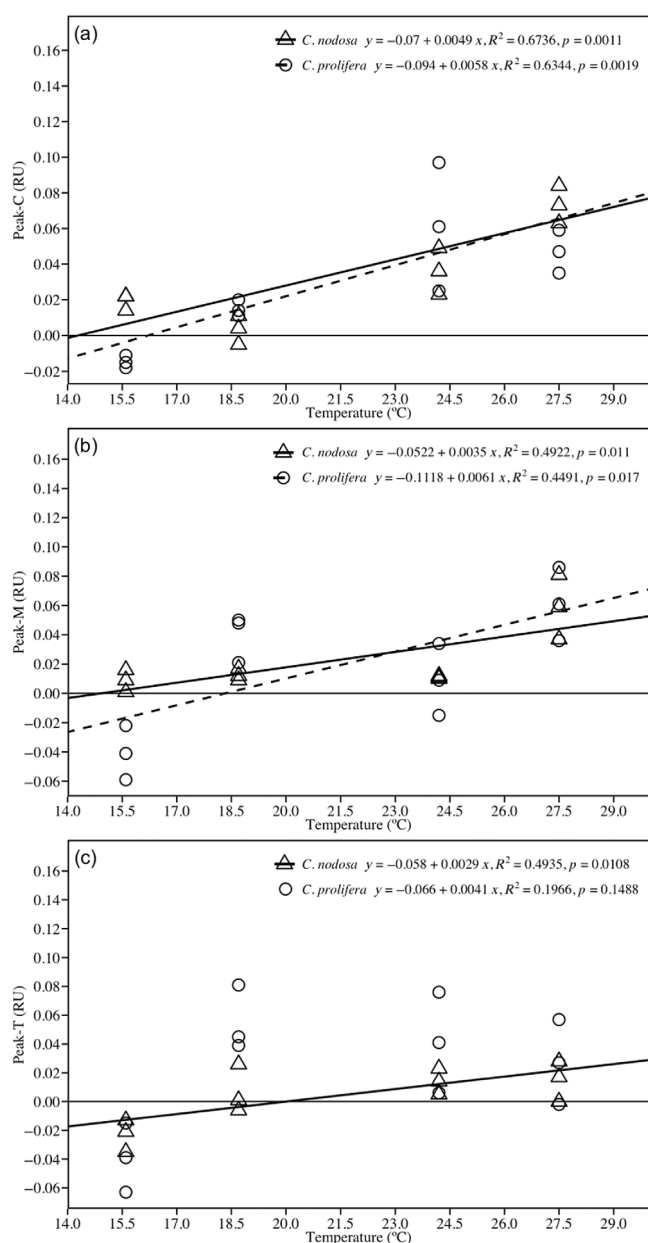


Fig. 7. Relationship between temperature with (a) fluorescent humic-like peak-C, (b) fluorescent humic-like peak-M and (c) fluorescent protein-like peak-T for each community. Solid and dotted lines represent significant linear regression for *Cymodocea nodosa* and *Caulerpa prolifera*, respectively.

production and bacterioplankton productivity recorded in some seagrass communities (Ziegler and Benner 1999; Ziegler et al. 2004) and with the high concentrations of easily degradable proteinaceous components found recently in a seagrass system (Akhand et al. 2021). Similarly, the high fraction of DOC_R found in our experiment may also explain the recalcitrant character of DOC released in other seagrass communities (Watanabe and Kuwae 2015; Jiménez-Ramos et al. 2022). On the other hand, while opportunistic macroalgal species usually release highly labile and biodegradable DOC (Zhang and

Wang 2017; Chen et al. 2020), other species like the kelp *Ecklonia cava* show a more recalcitrant character in released DOC (Wada et al. 2008; Zhang et al. 2017). Our results indicated that *C. prolifera* appears to release a high proportion of recalcitrant DOC in control treatments (87% in winter and 64% in summer). These results are in agreement with those obtained by optical characterization of the DOM produced. Our results suggest that humic-like fluorescence may dominate in vegetated coastal communities as the peak-T/peak-C ratio (Supporting Information Table S4), a measure of the ratio between protein-like and humic-like components, was less than 1 or negative in most treatments.

Our results on the recalcitrant DOC fraction have important implications for conservation and management, as they support the idea that vegetated coastal communities may not only contribute to ocean carbon sequestration as recalcitrant carbon buried in their sediments (Nellemann et al. 2009; Duarte et al. 2013), but also as recalcitrant carbon sequestered in dissolved form in the water column, similar to the recalcitrant DOC fraction of plankton in the open ocean (Jiao et al. 2010, 2014). However, the scaling-up of our DOC bioavailability assay results should be viewed with caution. There are multiple reasons why results under controlled laboratory conditions may not fully reflect the natural long-term fate of DOC released by these macrophytes. Recalcitrance may vary between different bacterial species, and different environments (Jiao et al. 2014; Watanabe et al. 2020). Although previous work on DOC bioavailability reached the stationary phase in DOC concentration within the incubation time used here (7 d; Jiménez-Ramos et al. 2022), some previous studies indicated that short-term degradation experiments may underestimate the long-term persistence of organic carbon (Trevathan-Tackett et al. 2020). Finally, there are DOC degradation processes that were not measured in this study (photochemical degradation) that could also be important in driving DOC degradation (Wada et al., 2015). Regardless, our study shows how seagrasses and macroalgae can directly release a significant fraction of nonlabile DOC, with a high potential to contribute to the recalcitrant fraction of oceanic DOC. This DOC can help counteract climate change through the fraction exported to deep waters, where it remains “trapped” long enough to qualify as sequestration, even if fully respired to CO₂ (Krause-Jensen and Duarte 2016). Furthermore, it should be noted that although marine prokaryotes consume labile DOC, they can also produce recalcitrant DOC as a metabolic by-product (Jiao et al. 2010). Therefore, long-term studies on the bioavailability of DOC released by macrophytes that include molecular fingerprints and carbon fluxes through the microbial loop are needed to better understand the role of DOC released by these important communities in climate regulation capacity.

One of the most remarkable results of this study was the increase in the fraction of recalcitrant DOC in both communities under marine heatwave conditions. Increase temperature also changed the quality (i.e., chemical structure) of DOM

produced by both communities, as indicated by the shift of Ex/Em humic-like maxima from longer (peak-C) to shorter wavelengths (peak-M). Moreover, a positive and significant correlation between humic-like substances and temperature for both communities were found (Fig. 7). This is probably due to both the increased production of recalcitrant DOC directly by the macrophytes themselves and the microbial transformation of labile to recalcitrant DOM by the marine prokaryotes. The production of recalcitrant DOC by macrophytes may be related to the production of secondary metabolites, as it is in summer (i.e., higher temperatures) that macrophytes increase secondary metabolism characterized by humic compounds (Rotini et al. 2013). Also, higher temperatures increase bacteria abundance, production and respiration (Joint and Smale 2017), which may drive the consumption of labile DOM by these marine prokaryotes, which may also produce recalcitrant DOM as a metabolic by-product (Jiao et al. 2010; Koch et al. 2013). These are hypotheses that need to be tested in future research. Increased release of recalcitrant DOC by macrophyte communities with increasing temperature has important conservation and management implications, especially for *C. nodosa*, as this study shows how increasing seawater temperature could not only enhance its productivity, but also increase the recalcitrant fraction of DOC produced.

Conclusions

The results of this study indicated that marine heatwaves can increase the productivity of seagrass-dominated communities such as *Cymodocea nodosa* and shift DOC fluxes from *Caulerpa prolifera*-dominated community to negative in summer. Our results also showed that both communities are highly DOC-producing, especially during sunlight hours for *C. nodosa* and dark hours for *C. prolifera*. *C. nodosa* produced a substantial amount of labile (58% and 44% in winter and summer, respectively) and recalcitrant (42% and 56% in winter and summer, respectively) DOC, whereas *C. prolifera* released mainly recalcitrant DOC (87% and 64% in winter and summer, respectively). This research also revealed that temperature is an important factor determining the chemical structure and bioavailability of DOC produced by these communities, as both vegetated coastal communities tend to produce more humic-like and less bioavailable DOC with increasing temperature. Finally, our results follow in line with previous studies highlighting the role of vegetated coastal communities in sequestering recalcitrant carbon in dissolved form in the ocean, adding further arguments to the growing need for their protection and conservation as valuable ecosystems to combat climate change now and under future global change scenarios.

Data availability statement

All relevant data are within the paper and its Supporting Information file.

References

- Akhand, A., and others. 2021. Lateral carbon fluxes and CO₂ evasion from a subtropical mangrove-seagrass-coral continuum. *Sci. Total Environ.* **752**: 142190. doi:10.1016/j.scitotenv.2020.142190
- Arias-Ortiz, A., and others. 2018. A marine heatwave drives massive losses from the world's largest seagrass carbon stocks. *Nat. Clim. Change* **8**: 338–344. doi:10.1038/s41558-018-0096-y
- Barrón, C., E. T. Apostolaki, and C. M. Duarte. 2014. Dissolved organic carbon fluxes by seagrass meadows and macroalgal beds. *Front. Mar. Sci.* **1**: 42. doi:10.3389/fmars.2014.00042
- Brun, F., I. Hernández, J. J. Vergara, G. Peralta, and J. L. Pérez-Lloréns. 2002. Assessing the toxicity of ammonium pulses to the survival and growth of *Zostera noltii*. *Mar. Ecol. Prog. Ser.* **225**: 177–187. doi:10.3354/meps225177
- Campagne, C. S., J.-M. Salles, P. Boissery, and J. Deter. 2015. The seagrass *Posidonia oceanica*: Ecosystem services identification and economic evaluation of goods and benefits. *Mar. Pollut. Bull.* **97**: 391–400. doi:10.1016/j.marpolbul.2015.05.061
- Carruthers, T. J. B., B. J. Longstaff, W. C. Dennison, E. G. Abal, and K. Aioi. 2001. Measurement of light penetration in relation to seagrass, p. 369–392. In F. T. Short and R. G. Coles [eds.], *Global seagrass research methods*. Elsevier Science BV.
- Champanois, W., and A. V. Borges. 2012. Seasonal and inter-annual variations of community metabolism rates of a *Posidonia oceanica* seagrass meadow. *Limnol. Oceanogr.* **57**: 347–361. doi:10.4319/lo.2012.57.1.0347
- Chen, J., H. Li, Z. Zhang, C. He, Q. Shi, N. Jiao, and Y. Zhang. 2020. DOC dynamics and bacterial community succession during long-term degradation of *Ulva prolifera* and their implications for the legacy effect of green tides on refractory DOC pool in seawater. *Water Res.* **185**: 116268. doi:10.1016/j.watres.2020.116268
- Coble, P. G. 1996. Characterization of marine and terrestrial DOM in seawater using excitation-emission matrix spectroscopy. *Mar. Chem.* **51**: 325–346. doi:10.1016/0304-4203(95)00062-3
- Coble, P. G., C. E. Del Castillo, and B. Avril. 1998. Distribution and optical properties of CDOM in the Arabian Sea during the 1995 Southwest Monsoon. *Deep Sea Res. Part II Top. Stud. Oceanogr.* **45**: 2195–2223. doi:10.1016/S0967-0645(98)00068-X
- Collier, C. J., S. Uthicke, and M. Waycott. 2011. Thermal tolerance of two seagrass species at contrasting light levels: Implications for future distribution in the Great Barrier Reef. *Limnol. Oceanogr.* **56**: 2200–2210. doi:10.4319/lo.2011.56.6.2200
- Deguette, A., I. Barrote, and J. Silva. 2022. Physiological and morphological effects of a marine heatwave on the seagrass *Cymodocea nodosa*. *Sci. Rep.* **12**: 7950. doi:10.1038/s41598-022-12102-x

- Duarte, C. M., H. Kennedy, N. Marbà, and I. Hendriks. 2013. Assessing the capacity of seagrass meadows for carbon burial: Current limitations and future strategies. *Ocean Coast. Manag.* **83**: 32–38. doi:10.1016/j.ocecoaman.2011.09.001
- Duarte, C. M., N. Marbà, E. Gacia, J. W. Fourqurean, J. Beggins, C. Barrón, and E. T. Apostolaki. 2010. Seagrass community metabolism: Assessing the carbon sink capacity of seagrass meadows. *Global Biogeochem. Cycl.* **24**: GB4032. doi:10.1029/2010GB003793
- Egea, L. G., R. Jiménez-Ramos, I. Hernández, T. J. Bouma, and F. G. Brun. 2018a. Effects of ocean acidification and hydrodynamic conditions on carbon metabolism and dissolved organic carbon (DOC) fluxes in seagrass populations. *PLoS One* **13**: e0192402. doi:10.1371/journal.pone.0192402
- Egea, L. G., R. Jiménez-Ramos, J. J. Vergara, I. Hernández, and F. G. Brun. 2018b. Interactive effect of temperature, acidification and ammonium enrichment on the seagrass *Cymodocea nodosa*. *Mar. Pollut. Bull.* **134**: 14–26. doi:10.1016/j.marpolbul.2018.02.029
- Egea, L. G., R. Jiménez-Ramos, I. Hernández, and F. G. Brun. 2019a. Effect of *in situ* short-term temperature increase on carbon metabolism and dissolved organic carbon (DOC) fluxes in a community dominated by the seagrass *Cymodocea nodosa*. *PLoS One* **14**: e0210386. doi:10.1371/journal.pone.0210386
- Egea, L. G., C. Barrón, R. Jiménez-Ramos, I. Hernández, J. J. Vergara, J. L. Pérez-Lloréns, and F. G. Brun. 2019b. Coupling carbon metabolism and dissolved organic carbon fluxes in benthic and pelagic coastal communities. *Estuar. Coast. Shelf Sci.* **227**: 106336. doi:10.1016/j.ecss.2019.106336
- Egea, L. G., R. Jiménez-Ramos, I. Hernández, and F. G. Brun. 2020. Differential effects of nutrient enrichment on carbon metabolism and dissolved organic carbon (DOC) fluxes in macrophytic benthic communities. *Mar. Environ. Res.* **162**: 105179. doi:10.1016/j.marenvres.2020.105179
- Ferguson, A. J. P., R. Gruber, J. Potts, A. Wright, D. T. Welsh, and P. Scanes. 2017. Oxygen and carbon metabolism of *Zostera muelleri* across a depth gradient—Implications for resilience and blue carbon. *Estuar. Coast. Shelf Sci.* **187**: 216–230. doi:10.1016/j.ecss.2017.01.005
- Godin, P., R. W. Macdonald, Z. Z. A. Kuzyk, M. A. Goñi, and G. A. Stern. 2017. Organic matter compositions of rivers draining into Hudson Bay: Present-day trends and potential as recorders of future climate change. *J. Geophys. Res. Biogeo.* **122**: 1848–1869. doi:10.1002/2016JG003569
- Hansell, D. A. 2013. Recalcitrant dissolved organic carbon fractions. *Ann. Rev. Mar. Sci.* **5**: 421–445. doi:10.1146/annurev-marine-120710-100757
- Harrison, X. A., and others. 2018. A brief introduction to mixed effects modelling and multi-model inference in ecology. *PeerJ* **6**: e4794. doi:10.7717/peerj.4794
- Hobday, A. J., and others. 2016. A hierarchical approach to defining marine heatwaves. *Prog. Oceanogr.* **141**: 227–238. doi:10.1016/j.pocean.2015.12.014
- Jiao, N., and others. 2010. Microbial production of recalcitrant dissolved organic matter: Long-term carbon storage in the global ocean. *Nat. Rev. Microbiol.* **8**: 593–599. doi:10.1038/nrmicro2386
- Jiao, N., and others. 2014. Mechanisms of microbial carbon sequestration in the ocean—Future research directions. *Biogeosciences* **11**: 5285–5306. doi:10.5194/bg-11-5285-2014
- Jiménez-Ramos, R., L. G. Egea, J. J. Vergara, and F. G. Brun. 2021. Factors modulating herbivory patterns in *Cymodocea nodosa* meadows. *Limnol. Oceanogr.* **66**: 2218–2233. doi:10.1002/lno.11749
- Jiménez-Ramos, R., F. Tomas, X. Reynés, C. Romera-Castillo, J. L. Pérez-Lloréns, and L. G. Egea. 2022. Carbon metabolism and bioavailability of dissolved organic carbon (DOC) fluxes in seagrass communities are altered under the presence of the tropical invasive alga *Halimeda incrassata*. *Sci. Total Environ.* **839**: 156325. doi:10.1016/j.scitotenv.2022.156325
- Joint, I., and D. A. Smale. 2017. Marine heatwaves and optimal temperatures for microbial assemblage activity. *FEMS Microbiol. Ecol.* **93**: fw243. doi:10.1093/femsec/fw243
- Kennedy, H., J. Beggins, C. M. Duarte, J. W. Fourqurean, M. Holmer, N. Marbà, and J. J. Middelburg. 2010. Seagrass sediments as a global carbon sink: Isotopic constraints. *Global Biogeochem. Cycl.* **24**: GB4026. doi:10.1029/2010GB003848
- Koch, M., G. Bowes, C. Ross, and X.-H. Zhang. 2013. Climate change and ocean acidification effects on seagrasses and marine macroalgae. *Glob. Chang. Biol.* **19**: 103–132. doi:10.1111/j.1365-2486.2012.02791.x
- Krause-Jensen, D., and C. M. Duarte. 2016. Substantial role of macroalgae in marine carbon sequestration. *Nat. Geosci.* **9**: 737–742. doi:10.1038/ngeo2790
- Larsen, S., T. Andersen, and D. O. Hessen. 2011. Climate change predicted to cause severe increase of organic carbon in lakes. *Glob. Change Biol.* **17**: 1186–1192. doi:10.1111/j.1365-2486.2010.02257.x
- Lawaetz, A. J., and C. A. Stedmon. 2009. Fluorescence intensity calibration using the Raman scatter peak of water. *Appl. Spectrosc.* **63**: 936–940. doi:10.1366/000370209788964548
- Lenth, R., H. Singmann, J. Love, P. Buerkner, and M. Herve. 2019. Emmeans: Estimated marginal means, aka least-squares means. R Package (2019), Version 1.3.3.
- Liu, S., Y. Deng, Z. Jiang, Y. Wu, X. Huang, and P. I. Macreadie. 2020. Nutrient loading diminishes the dissolved organic carbon drawdown capacity of seagrass ecosystems. *Sci. Total Environ.* **740**: 140185. doi:10.1016/j.scitotenv.2020.140185
- Loginova, A. N., A. W. Dale, F. A. C. Le Moigne, S. Thomsen, S. Sommer, D. Clemens, K. Wallmann, and A. Engel. 2020. Sediment release of dissolved organic matter to the oxygen

- minimum zone off Peru. *Biogeosciences* **17**: 4663–4679. doi:10.5194/bg-17-4663-2020
- Macreadie, P., and S. Hardy. 2018. Response of seagrass “blue carbon” stocks to increased water temperatures. *Diversity* **10**: 115. doi:10.3390/d10040115
- Malinverno, A., and E. A. Martinez. 2015. The effect of temperature on organic carbon degradation in marine sediments. *Sci. Rep.* **5**: 17861. doi:10.1038/srep17861
- Marsh, J. A., W. C. Dennison, and R. S. Alberte. 1986. Effects of temperature on photosynthesis and respiration in eelgrass (*Zostera marina* L.). *J. Exp. Mar. Biol. Ecol.* **101**: 257–267. doi:10.1016/0022-0981(86)90267-4
- Murphy, K. R., K. D. Butler, R. G. M. Spencer, C. A. Stedmon, J. R. Boehme, and G. R. Aiken. 2010. Measurement of dissolved organic matter fluorescence in aquatic environments: An interlaboratory comparison. *Environ. Sci. Technol.* **44**: 9405–9412. doi:10.1021/es102362t
- Murphy, K. R., C. A. Stedmon, D. Graeber, and R. Bro. 2013. Fluorescence spectroscopy and multi-way techniques. *PARAFAC. Anal. Methods* **5**: 6557. doi:10.1039/c3ay41160e
- Navarro, N., S. Agustí, and C. M. Duarte. 2004. Plankton metabolism and DOC use in the Bay of Palma, NW Mediterranean Sea. *Aquat. Microb. Ecol.* **37**: 1–24. doi:10.3354/ame037047
- Nellemann, C., E. Corcoran, C. M. Duarte, L. Valdés, C. De Young, L. Fonseca, and G. Grimsditch. 2009. Blue carbon: The role of healthy oceans in binding carbon. A rapid response assessment. United Nations Environment Programme, GRID-Arendal.
- Olivé, I., J. Silva, M. M. Costa, and R. Santos. 2016. Estimating seagrass community metabolism using benthic chambers: The effect of incubation time. *Estuar. Coast.* **39**: 138–144. doi:10.1007/s12237-015-9973-z
- Oliver, E. C. J., and others. 2019. Projected marine heatwaves in the 21st century and the potential for ecological impact. *Front. Mar. Sci.* **6**: 734. doi:10.3389/fmars.2019.00734
- Pai, S.-C., G.-C. Gong, and K.-K. Liu. 1993. Determination of dissolved oxygen in seawater by direct spectrophotometry of total iodine. *Mar. Chem.* **41**: 343–351. doi:10.1016/0304-4203(93)90266-Q
- Peralta, G., and others. 2021. The morphometric acclimation to depth explains the long-term resilience of the seagrass *Cymodocea nodosa* in a shallow tidal lagoon. *J. Environ. Manage.* **299**: 113452. doi:10.1016/j.jenvman.2021.113452
- Roland, F., N. F. Caraco, J. J. Cole, and P. del Giorgio. 1999. Rapid and precise determination of dissolved oxygen by spectrophotometry: Evaluation of interference from color and turbidity. *Limnol. Oceanogr.* **44**: 1148–1154. doi:10.4319/lo.1999.44.4.1148
- Rotini, A., A. Belmonte, I. Barrote, C. Micheli, A. Peirano, R. O. Santos, J. Silva, and L. Migliore. 2013. Effectiveness and consistency of a suite of descriptors for assessing the ecological status of seagrass meadows (*Posidonia oceanica* L. Delile). *Estuar. Coast. Shelf Sci.* **130**: 252–259. doi:10.1016/j.ecss.2013.06.015
- Savva, I., S. Bennett, G. Roca, G. Jordà, and N. Marbà. 2018. Thermal tolerance of Mediterranean marine macrophytes: Vulnerability to global warming. *Ecol. Evol.* **8**: 12032–12043. doi:10.1002/ece3.4663
- Schlegel, R. W. 2020. Marine heatwave tracker. <http://www.marineheatwaves.org/tracker>
- Stedmon, C. A., and R. Bro. 2008. Characterizing dissolved organic matter fluorescence with parallel factor analysis: A tutorial. *Limnol. Oceanogr. Methods* **6**: 572–579. doi:10.4319/lom.2008.6.572
- Terrados, J., and J. D. Ros. 1992. The influence of temperature on seasonal variation of *Caulerpa prolifera* (Forsskal) Lamouroux photosynthesis and respiration. *J. Exp. Mar. Bio. Ecol.* **162**: 199–212. doi:10.1016/0022-0981(92)90201-K
- Terrados, J., and J. D. Ros. 1995. Temperature effects on photosynthesis and depth distribution of the seagrass *Cymodocea nodosa* (ucris) Ascherson in a Mediterranean coastal lagoon: The Mar Menor (SE Spain). *Mar. Ecol.* **16**: 133–144. doi:10.1111/j.1439-0485.1995.tb00400.x
- Tovar, A., C. Moreno, M. P. Manuel-Vez, and M. García-Vargas. 2000. Environmental impacts of intensive aquaculture in marine waters. *Water Res.* **34**: 334–342. doi:10.1016/S0043-1354(99)00102-5
- Trevathan-Tackett, S. M., T. C. Jeffries, P. I. Macreadie, B. Manojlovic, and P. Ralph. 2020. Long-term decomposition captures key steps in microbial breakdown of seagrass litter. *Sci. Total Environ.* **705**: 135806. doi:10.1016/j.scitotenv.2019.135806
- Tuya, F., L. Png-Gonzalez, R. Riera, R. Haroun, and F. Espino. 2014. Ecological structure and function differs between habitats dominated by seagrasses and green seaweeds. *Mar. Environ. Res.* **98**: 1–13. doi:10.1016/j.marenvres.2014.03.015
- Vaquer-Sunyer, R., and C. M. Duarte. 2008. Thresholds of hypoxia for marine biodiversity. *Proc. Natl. Acad. Sci.* **105**: 15452–15457. doi:10.1073/pnas.0803833105
- Vaquer-Sunyer, R., C. M. Duarte, G. Jordà, and S. Ruiz-Halpern. 2012. Temperature dependence of oxygen dynamics and community metabolism in a shallow mediterranean macroalgal meadow (*Caulerpa prolifera*). *Estuar. Coast.* **35**: 1182–1192. doi:10.1007/s12237-012-9514-y
- Vergara, J. J., M. P. García-Sánchez, I. Olivé, P. García-Marín, F. G. Brun, J. L. Pérez-Lloréns, and I. Hernández. 2012. Seasonal functioning and dynamics of *Caulerpa prolifera* meadows in shallow areas: An integrated approach in Cadiz Bay Natural Park. *Estuar. Coast. Shelf Sci.* **112**: 255–264. doi:10.1016/j.ecss.2012.07.031
- Wada, S., M. Aoki, A. Mikami, T. Komatsu, Y. Tsuchiya, T. Sato, H. Shinagawa, and T. Hama. 2008. Bioavailability of macroalgal dissolved organic matter in seawater. *Mar. Ecol. Prog. Ser.* **370**: 33–44. doi:10.3354/meps07645

- Wada, S., Y. Omori, Y. Kayamyo, Y. Tashiro, and T. Hama. 2015. Photoreactivity of dissolved organic matter from macroalgae. *Reg. Stud. Mar. Sci.* **2**: 12–18. doi:[10.1016/j.rsma.2015.08.018](https://doi.org/10.1016/j.rsma.2015.08.018)
- Watanabe, K., and T. Kuwae. 2015. How organic carbon derived from multiple sources contributes to carbon sequestration processes in a shallow coastal system? *Global Change Biol.* **21**: 2612–2623. doi:[10.1111/gcb.12924](https://doi.org/10.1111/gcb.12924)
- Watanabe, K., G. Yoshida, M. Hori, Y. Umezawa, H. Moki, and T. Kuwae. 2020. Macroalgal metabolism and lateral carbon flows can create significant carbon sinks. *Biogeosciences* **17**: 2425–2440. doi:[10.5194/bg-17-2425-2020](https://doi.org/10.5194/bg-17-2425-2020)
- Weigel, B. L., and C. A. Pfister. 2021. The dynamics and stoichiometry of dissolved organic carbon release by kelp. *Ecology* **102**: e03221. doi:[10.1002/ecy.3221](https://doi.org/10.1002/ecy.3221)
- Wernberg, T., D. A. Smale, F. Tuya, M. S. Thomsen, T. J. Langlois, T. de Bettignies, S. Bennett, and C. S. Rousseaux. 2013. An extreme climatic event alters marine ecosystem structure in a global biodiversity hotspot. *Nat. Clim. Change* **3**: 78–82. doi:[10.1038/nclimate1627](https://doi.org/10.1038/nclimate1627)
- Xu, K., M. Li, W. Wang, Y. Xu, D. Ji, C. Chen, and C. Xie. 2022. Differences in organic carbon release between conchocelis and thalli of *Pyropia haitanensis* and responses to changes in light intensity and pH. *Algal Res.* **61**: 102574. doi:[10.1016/j.algal.2021.102574](https://doi.org/10.1016/j.algal.2021.102574)
- Yamashita, Y., and E. Tanoue. 2008. Production of bio-refractory fluorescent dissolved organic matter in the ocean interior. *Nat. Geosci.* **1**: 579–582. doi:[10.1038/ngeo279](https://doi.org/10.1038/ngeo279)
- Zhang, T., and X. Wang. 2017. Release and microbial degradation of dissolved organic matter (DOM) from the macroalgae *Ulva prolifera*. *Mar. Pollut. Bull.* **125**: 192–198. doi:[10.1016/j.marpolbul.2017.08.029](https://doi.org/10.1016/j.marpolbul.2017.08.029)
- Zhang, Y., and others. 2017. Carbon sequestration processes and mechanisms in coastal mariculture environments in China. *Sci. China Earth Sci.* **60**: 2097–2107. doi:[10.1007/s11430-017-9148-7](https://doi.org/10.1007/s11430-017-9148-7)
- Ziegler, S., and R. Benner. 1999. Dissolved organic carbon cycling in a subtropical seagrass-dominated lagoon. *Mar. Ecol. Prog. Ser.* **180**: 149–160. doi:[10.3354/meps180149](https://doi.org/10.3354/meps180149)
- Ziegler, S., E. Kaiser, and R. Benner. 2004. Dynamics of dissolved organic carbon, nitrogen and phosphorus in a seagrass meadow of Laguna Madre, Texas. *Bull. Mar. Sci.* **75**: 391–407.

Acknowledgments

This study has been supported by the Spanish National Project PAVAROTTI (CTM2017-85365-R); by SER-CADY project (FEDER-UCA18-107451). This project was co-financed by the European Union under the 2014–2020 ERDF Operational Programme and by the Department of Economic Transformation, Industry, Knowledge, and Universities of the Regional Government of Andalusia; by the Spanish National Project RECOUNT (PID2020-120237RJ-I00). This project was financed by MCIN/AEI/10.13039/501100011033. The authors thank Enaitz Aguirre, Sergio Barro and Asier Ibáñez (Aquatic-Biotechnology) for field assistance. The authors thank the three anonymous referees for their constructive comments on an early version of the manuscript. Finally, our thanks to the Integration and Application Network for the courtesy of supplying vector symbols (<https://ian.umces.edu/media-library/symbols/>).

Conflict of Interest

None declared.

Submitted 22 December 2021

Revised 26 October 2022

Accepted 24 November 2022

Associate editor: Elizabeth B Kujawinski